ISSN 2347-3487
Volume 14 Number 1
Journal of Advances in Physics

Newly discovered Topological Insulator Sr_3SnO for Spintronics, Optical and Electronic properties

Rasha W. Adnan Moh'd, Juwayni Lucman, Faris Mahmoud Safieh, Noureddine Amrane* and Maamar Benkraouda

Department of Physics
United Arab Emirates University, Al-Ain, P.O. Box: 15551, U.A.E.

ABSTRACT

A theoretical study of the electronic and optical properties of dilute magnetic semiconductor Sr_3SnO is presented, using the full potential linearized augmented plane wave method. The Perdew Burke Ernzerhof (GGA08) (generalized gradient approximation) is used for the total energy calculations, while the Modified Becke–Johnson (MBJ) is used for electronic structure calculations since this functional was designed to reproduce as well as possible the exact exchange correlation potential rather than the total energy, and as a result gives significantly improved results such as band gap and electronic structure. In this study, we have investigated the optical properties by means of first-principles density-functional total-energy calculation using the all-electron full potential linear augmented plane-wave method (FPLAPW).

Kreywords: Band structure, dielectric function, refractive index.

*Corresponding author: Noureddine Amrane,

Email: namrane@uaeu.ac.ae

INTRODUCTION

Researchers at North Carolina State University have created a new compound that can be integrated into silicon chips and is a dilute magnetic semiconductor [1,2], meaning that it could be used to make "spintronic" devices, which rely on magnetic force to operate, rather than electrical currents.

The researchers synthesized the new compound, strontium tin oxide (Sr_3SnO), as an epitaxial thin film on a silicon chip.

The new material is a significant step forward in the field of spin-based electronics or "spintronics" where the spin state of electrons is exploited to carry, manipulate and store information. Conventional electronic circuits use only the charge state (current on or off) of an electron, but these tiny particles also have a spin direction (up or down).

This relatively new field of semiconductor spintronics [3,4] seeks to exploit the spin of charge carriers in new generations of transistors, lasers and integrated magnetic sensors. The ability to control the spin injection, transport and detection leads to the potential for new classes of ultra-low power, high speed memory, logic and photonic devices, novel devices such as spin-polarized light emitters and spin field effect transistors. It is widely expected that new functionalities for electronics and photonics can be derived if the injection, transfer and detection of carrier spin can be controlled above room temperature. Among this new class of devices are spin transistors operating at very low powers for mobile applications that rely on batteries, optical emitters with encoded information through their polarized light output, fast non-volatile semiconductor memory and integrated magnetic/electronic/photonic devices (''electromagnetism-on-a-chip'').

The recent prediction of non-layered inverse-perovskites based structure to exhibit a strong topological insulator (TI) electronic state motivated both theory and experimental community to investigate this class of material [5-7]. Pervoskites materials are interesting due to the fact they do host a variety of materials properties such as spin dependent transport, superconductivity, Ferroelectricity and colossal magnetoresistance. The advantage is in the ability to build a perfect heterostructure system without any lattice distortion. From future application point of view the interface between superconductor and topological insulator will lead to the realization of Majorano fermions, which play an essential role in topological quantum computer [8].

Y. F. Lee et al [9-11] successfully managed to grow epitaxial Sr3SnO (SSO) one of the predicted TI film on Si based substrate by means of pulsed leaser deposition (PLD). The new inverse-perovskites (SSO) turned to exhibit a ferromagnetic state at room temperature, which will pave the way toward integrating the spin degree of freedom in silicon based electronic devices. One of the limitation is the epitaxial growth, which is carried via PLD; this is not suitable for large wafer deposition. We propose to grow high quality epitaxial SSO structure by ultra-high vacuum sputtering system. Sputtering a widely used large-scale deposition

technique. Recently under well controlled growth condition H. L. Wang et al. [12,13] managed to grow epitaxial ferromagnetic insulator high quality Yttrium Iron Garnet (YIG) film.

In this work, we use the Generalized Gradient Approximation (GGA) method to make detailed theoretical investigations on Sr_3SnO.

In this work, we have investigated the electronic and optical properties of Sr3SnO compound by means of first-principles density-functional total-energy calculation using the all-electron full potential linear augmented plane-wave method (FP-LAPW). The energy bands along high symmetry directions. The accurate calculations of linear optical function (refractive index, reflectance, coefficient of absorption, and both imaginary and real dielectric function) is performed in the photon energy range up to 15 eV.

The rest of the paper is organized as follows. In Section 2, we describe the computational method used in the present work. Results about the electronic properties are presented in Section 3. A conclusion of the work is given in Section 4.

CALCULATIONS

Scalar relativistic calculations have been performed using the wien2k code [14,15]. For the exchange correlation potential, we have used the local density approximation (LDA) with a parameterization of Ceperly-Adler data [16]. The new Full Potential Augmented Plane Wave method of the density functional theory is applied [17,18]. Several improvements to solve the energy dependence of the basis set were tried but the first really successful one was the linearization scheme introduced by Andersen [19] leading to the linearized augmented plane wave (LAPW) method. In LAPW, the energy dependence of each radial wave function inside the atomic sphere is linearized by taking a linear combination of a solution u at a fixed linearization energy and its energy derivative $\dot{u}$ computed at the same energy.

$$\Phi_K(\mathbf{r}) = \begin{cases} \sum_L \left[a_L^{\alpha \mathbf{K}} u_l^{\alpha}(r') + b_L^{\alpha \mathbf{K}} \dot{u}_l^{\alpha}(r') \right] Y_L(\hat{r}') & r' \langle R_\alpha \\ \Omega^{-1/2} \exp\left(i(k+K).r\right) & r \in I \end{cases} \quad (1)$$

Where $r'=r-r_\alpha$ is the position inside sphere α with polar coordinates r′ and r, **k** is a wave vector in the irreducible Brillouin zone, **K** is a reciprocal lattice vector and u_l^{α} is the numerical solution to the radial Schrodinger equation at the energy u_l ε. The coefficients $a_L^{\alpha K}$ are chosen such that the atomic functions

for all L components match (in value) the PW with K at the Muffin tin sphere boundary. The KS orbitals are expressed as a linear combination of APWs $\Phi_K(r)$. In 1991, Singh [20] introduced the concept of local orbitals (LOs) which allow an efficient treatment of the semi-core states. An LO is constructed by the LAPW radial functions u and $\dot{u}$ at one energy ε_1 in the valence band region and a third radial function at ε_2.

$$\Phi_{LO}(\mathbf{r}) = \begin{cases} \left[a_L^{\alpha,LO} u_{1l}^{\alpha}(\mathbf{r}') + b_L^{\alpha,LO} \dot{u}_{1l}^{\varepsilon}(\mathbf{r}') + c_L^{\alpha,LO} u_{2l}^{\alpha}(\mathbf{r}') \right] Y_L(\hat{r}') & r' \langle R_\alpha \\ 0 & r \in I \end{cases} \quad (2)$$

Recently, an alternative approach was proposed by Sjöstedt et al [21], namely the APLW + lo (local orbital) method. Here the augmentation is similar to the original APW scheme but each radial wave function is computed at a fixed linearization energy to avoid the non-linear eigenvalue problem. The missing variational freedom of the radial wave functions can be recovered by adding another type of local orbitals (termed in lower case to distinguish them from LO) containing u and $\dot{u}$ term:

$$\Phi_{lo}(\mathbf{r}) = \begin{cases} \left[a_L^{\alpha,lo} u_l^{\alpha}(\mathbf{r}') + b_L^{\alpha,lo} \dot{u}_l^{\alpha}(\mathbf{r}') \right] Y_L(\mathbf{r}') & r' \langle R_\alpha \\ 0 & r \in I \end{cases} \quad (3)$$

It was demonstrated that this new scheme converges faster than LAPW. The APW +lo scheme has been implemented in the wien2k code version [22].

However, in the calculations reported here, we chose the muffin tin radii for Sr, Sn and O to be 2.1 a.u.. The expansion of the spherical region is developed up to l_{max}=10, while in the interstitial region we have used 457 plane waves. Furthermore, we have used the energy cut-off of $R_{MT}.K_{max}$=8 and the maximal reciprocal vector equal to 10.

The integrals over the Brillouin zone are performed using the Monkorst-pack special k-points approach [23]. Since calculations of the optical properties require a denser k-matrix, we have used 1000 k-points in the irreducible Brillouin zone for integration in reciprocal space.

Optical properties of a solid are usually described in terms of the complex dielectric function $\varepsilon(\omega) = \epsilon_1(\omega) + i\varepsilon_2(\omega)$. The dielectric function is determined mainly by the transition between the valence and conduction bands according to perturbation theory; the imaginary part of the dielectric function in the

long wavelength limit has been obtained directly from the electronic structure calculation, using the joint density of states (DOS) and the optical matrix elements. It is expressed as

$$\varepsilon_2(\omega) = \frac{4\pi^2 e^2}{3m^2\omega^2} \sum_{l,n} \int_{BZ} \frac{2}{(2\pi)^3} d^3k \left|P_{nl}\right|^2 .\delta\left[E_l(k) - E_n(k) - \hbar\omega\right] \quad (4)$$

Where m is the mass and e the electrical charge of the electron, $\Sigma_{l.n}$ means the summation between all the conduction bands (l) and valence bands (n); and P_{nl} expresses the momentum matrix element between l and n. It is given by

$$P_{nl} = \frac{m}{\hbar}\left\langle nk\left|\nabla_k H,(k)\right|lk\right\rangle \quad (5)$$

Where H(k) is the Hamiltonian, and $\langle nk|,|lk\rangle$ are the k-space wave-functions. Using the FP-LAPW parameters, we can directly calculate P_{nl}.

The real part of the dielectric function can be derived from the imaginary part by the Kramers-Kronig relationship. The knowledge of both the real and the imaginary parts of the dielectric allows the calculation of important optical functions. In this paper, we also present and analyze the refractive index $n(\varpi)$ given by

$$n(\omega) = \left[\frac{\varepsilon_1(\omega)}{2} + \frac{\sqrt{\varepsilon_1^2(\omega) + \varepsilon_2^2(\omega)}}{2}\right]^{1/2} \quad (6)$$

At low frequency (ω=0), we get the following relation:

$$n(0) = \varepsilon^{1/2}(0) \quad (7)$$

To correct the LDA error in the band gaps a constant potential was applied to the conduction band states (using the scissors operator which rigidly shifts the conduction band states) in order to match the calculated band gaps with the experimental data.

RESULTS

The structural optimization of the cubic phase was performed by calculating the total energy as function of the volume. The minimization of the total energy versus volume requires that each of the self-consistent calculations converge, so the iteration process was repeated until the calculated total energy of the crystal converged to less than 1 mRyd. A total of nine iterations was necessary to achieve self-consistency.

The energy bands calculated for the k points along the high symmetry lines are shown in figures 1 and 2. The band gap is found to be direct and equal to 1.2 eV and 0.316 eV at the Γ point, using the Generalized gradient approximation and the Modified Becke-Johnson respectively, this is in close agreement with other theoretical calculations [24].

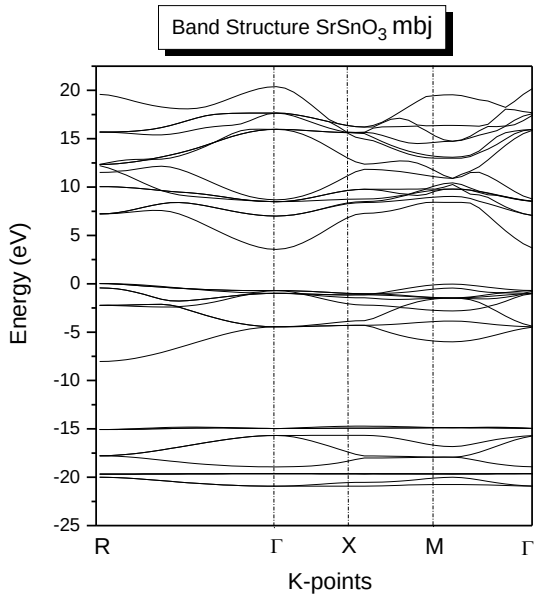

Figure 1

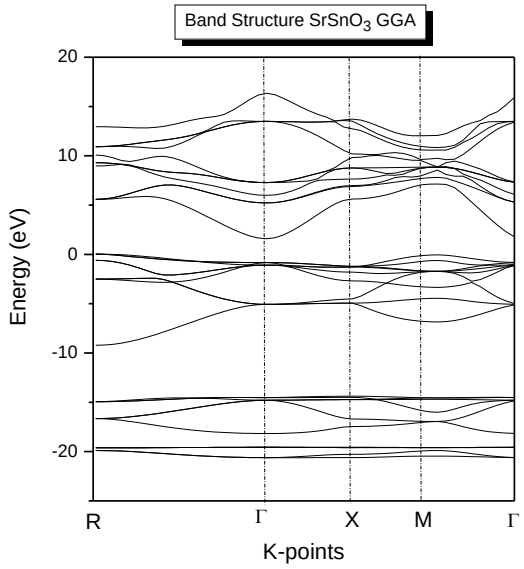

Figure 2

It is interesting to compare our calculated gaps with experimental data. Since quasi-particle excitations are not taken into account in density functional theory (DFT), the energy gap calculated from DFT, often called the Kohn-Sham gap, tends to be smaller than the experimental one.

In some cases, even the wrong ground state is predicted, as, e.g., in Ge, where the energy gap is around 0.7 eV, whereas the LDA Kohn-Sham gap is slightly negative at ambient pressure [25]. The GGA corrections yield only minor improvement. Quasiparticle calculations essentially overcome the

underestimate of the band gap as obtained using the LDA, The GW [26] calculations for GaN for instance yield band structures in much better agreement with experiment; they are, however, time consuming and do not, as yet, produce self-consistent total-energy values. However, in our case, the use the Modified Becke Johnson potential improves significantly the band gapwhich becomes closer to the experimental one.

The study of the optical constants and their variation with frequency is very interesting for the uses of films in optical applications. These applications require accurate knowledge of the optical constants over a wide wavelength range.

The reflectivity (R) of materials of refractive index (n) and extinction coefficient (k) is given by:

$$R = \frac{(n-1)^2 + k}{(n+1)^2 - k} \qquad (8)$$

The spectra of all optical functions were calculated in the spectrum range 0–15 eV. The dielectric functions of Sr_3SnO in the cubic structure are resolved into one component $\varepsilon_{xy}(\omega)$, Figures 3 shows the variation of the dispersive part of the dielectric function, ε_1.

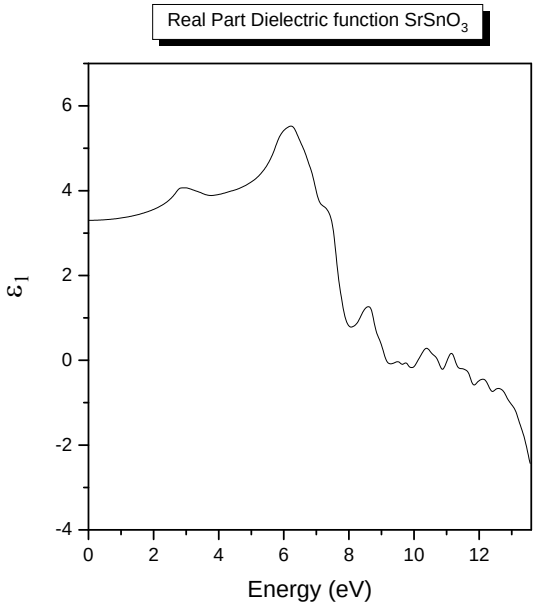

Figure 3

The calculated spectra have been obtained by Kramers-Kronig transformation of the shifted ε_2 spectra. The main features are a shoulder at lower energies, a rather steep decrease between 6.5 and 7.5 eV, after which ε_1 becomes negative, a minimum and a slow increase toward zero at higher energies.

ISSN 2347-3487
Volume 14 Number 1
Journal of Advances in Physics

Next, we consider the imaginary part of the electronic dielectric function for Sr_3SnO (see Figure 4), for radiation up to 15 eV. The calculated results are rigidly shifted upwards by 0.72 eV. The main feature is a broad peak with a maximum around 8 eV, the maximum amplitude is at 6.5, a shoulder is also visible at around 9 eV. The peak as well as the shoulders are excellently reproduced in the calculations, as are the general form of some experimental spectra [27]. There are also two other groups of peaks, in (9.5 eV- 12.5 eV) for Sr_3SnO photon energy range, they are mainly due to transitions in the vicinity of X and R.

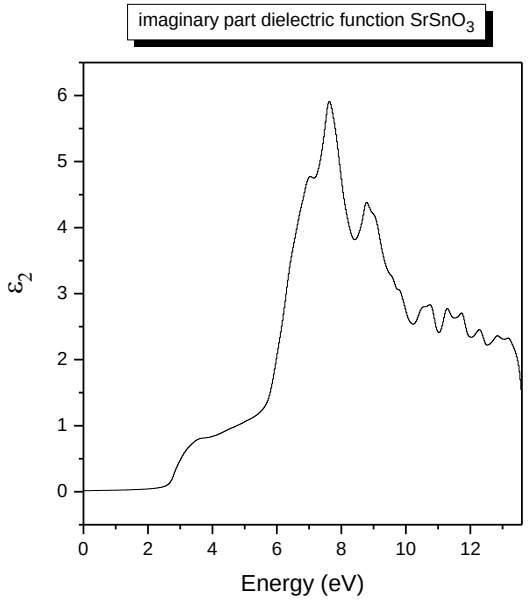

Figure 4

Figure 5 shows the reflectivity spectra in the energy region below 15 eV. The spectra are consistent with some previous measurements [28].

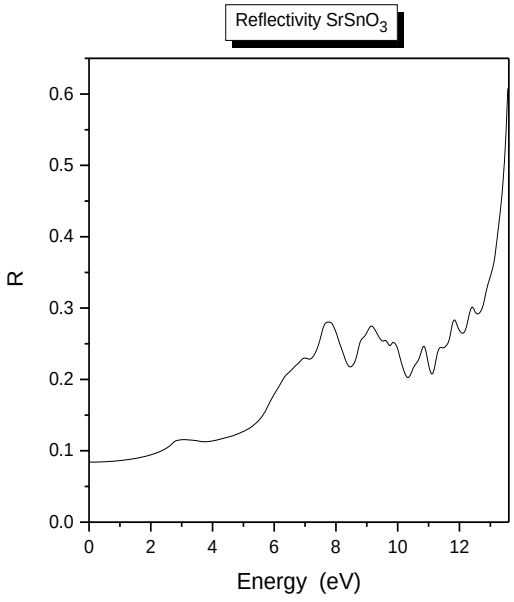

Figure 5

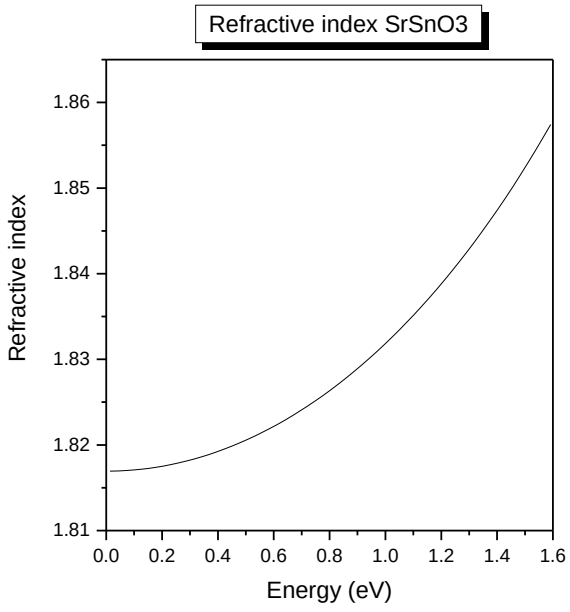

Figure 6

As seen in figure 6, the refractive index was computed using both real and imaginary parts of the dielectric function. It shows that the refractive index exhibits a significant dispersion in the short wavelength region were absorption is strong. It increases with the increase of the energy of the incident light, becoming nearly flat in the higher region.

Figure 7 shows the variation of the coefficient of extinction in the energy region below 15 eV, the extinction coefficient was found to increase with increasing photon energy for Sr_3SnO.

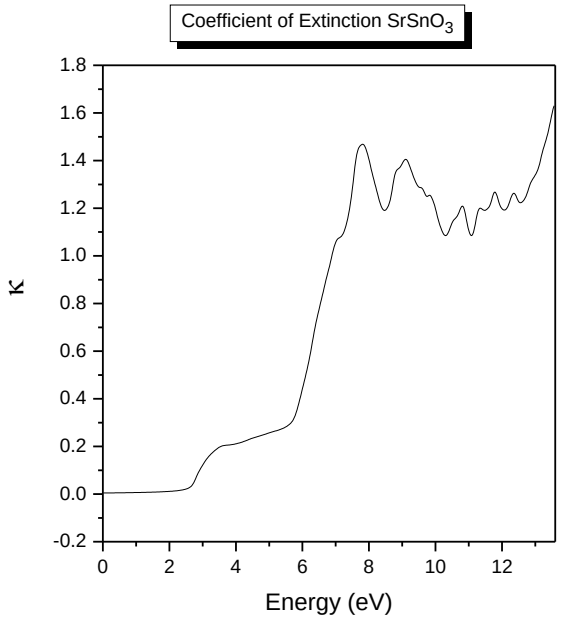

Figure 7

CONCLUSION

The electronic properties of Sr_3SnO compound have been investigated using the wien2k package. Full-potential linearized augmented plane wave (FP-LAPW) approach within the density functional theory (DFT) in the local density approximation (LDA) including the generalized gradient approximation (GGA) was used. The use of GGA92 and GGA96 for the exchange-correlation potential allows only minor improvements to the band gap, while the Modified Becke-Johnson scheme permitted us to obtain an energy gap, in good agreement with the experimental measurement and other theoretical calculations. The LDA-eigenvalue spectrum gives an excellent description of the band structures.

The optical properties of cubic Sr_3SnO have also been investigated, the real and imaginary parts of the dielectric functions were calculated for polarization in the x-y plane, the optical properties are excellently

reproduced using the density functional theory, if we allow for a rigid shift of the band structure, the so-called scissors operator. Thus, in this paper, all the optical spectra, and localization of transitions in the volume of the Brillouin zone are successfully calculated using the theoretical FLAPW method.

ACKNOWLEDGMENTS

We thank UAEU for their financial support through the Summer Undergraduate Research Experience Program (SURE PLUS 2017) Grant:G00002411

REFERENCES

1. Y. F. Lee, F. Wu, R. Kumar, F. Hunte, J. Schwartz and J. Narayan
   Epitaxial integration of dilute magnetic semiconductor Sr3SnO with Si (001), Appl. Phys. Lett. 103, 112101 (2013).
2. Yi-Fang Lee, Justin Schwartz, J. Narayan
   Tunable electronic structure in dilute magnetic semiconductor Sr3SnO/c-YSZ/Si (001) epitaxial Heterostructures, JOURNAL OF APPLIED PHYSICS 116, 164903 (2014)
3. David D. Awschalom and Michael E. Flatté, Challenges for semiconductor spintronics,
   Nature Physics 3, 153 - 159 (2007)
4. M. Idrish Miah, Generation and Detection of Spin Current in Semiconductors: Semiconductor Spintronics, Volume 2, Issue 10, Part B, 2015, Pages 5111–5116
5. M. Klintenberg, arXiv preprint arXiv: 1007.4838 (2010).
6. T. Das and A. V. Balatsky, Nature communications 4 (2013).
7. T. Kariyado and M. Ogata, Journal of the Physical Society of Japan 80 (8) (2011).
8. L. Fu and C. L. Kane, Physical Review Letters 100 (9), 096407 (2008).
9. Y. Lee, F. Wu, R. Kumar, F. Hunte, J. Schwartz and J. Narayan, Applied Physics Letters 103 (11), 112101 (2013).
10. Y. Lee, F. Wu, J. Narayan and J. Schwartz, MRS Communications 4 (01), 7-13 (2014).
11. Y. Lee, J. Narayan and J. Schwartz, Journal of Applied Physics 116 (16), 164903 (2014).
12. H. Wang, C. Du, Y. Pu, R. Adur, P. Hammel and F. Yang, Physical review letters 112 (19), 197201 (2014).
13. H. L. Wang, C. H. Du, Y. Pu, R. Adur, P. C. Hammel and F. Y. Yang, Physical Review B 88 100406 (2013).
14. K.Schwarz, P.Blaha, G.K.H.Madsen, Comput.Phys.Commun. 147 (2002) 71
15. K.Schwarz, P.Blaha, Comput.Mater.Sci. 28 (2003) 259
16. D.M.Ceperley, B.I.Alder, Phys.Rev.Lett.45 (1990) 566
17. E.Wimmer, H.Krakauer, M.Weinert, A.J.Freeman, Phys.Rev.B24 (1981) 864

18. P.Blaha, K.Schwarz, P.Sorantin, S.B.Trikey, Comput.Phys.Commun.59 (1990) 399
19. O.K.Andersen, Phys.Rev.B12 (1975) 3060-3083
20. D.Singh, Phys.Rev.B 43 (1991) 6388-6392
21. E.Sjöstedt, L.Nordström, D.J.Singh, Solid State Comm.114 (2000) 15-20
22. P.Blaha, K.Schwarz, G.K.H.Madsen, D.Kvanicka, J.Luitz, WIEN2k, An Augmented Plane Wave Plus Local Orbitals Program For Calculating Crystal properties, Vienna University of Technology,Austria 2001.
23. H.J.Monkhorst, J.D.Pack, Phys.Rev.B13 (1976) 5188
24. Y. F. Lee, J. Narayan, and J. Schwartz, Journal of Applied Physics 116, 164903 (2014)
25. M.Alouani and J.M.Wills, Phys.Rev.B54, 2480 (1996)
26. S. Taioli, P. Umari, M. M. De Souza, Phys. Stat. sol. (b) Vol. 246 Issue 11-12, 2572 – 2576
27. Vassilios Yannopapas and Alexander Moroz, J. Phys.: Condens. Matter 17 (2005) 3717–3734.
28. M. Ueta, H. Kanzaki, K. Kobayashi, Y. Toyozawa and E. Hanamura, Excitonic Processes in Solids, ed. M. Cardona, P. Fulde, K. von Klitzing and H.-J. Queisser (Springer, Berlin, 1986) Springer Ser. Solid-State Sci. 60, p.370.